Characterization of the Formation of the Pyrrole Moiety during Clorobiocin and Coumermycin A_1 Biosynthesis†

Sylvie Garneau,‡ Pieter C. Dorrestein,§ Neil L. Kelleher,§ and Christopher T. Walsh*,‡

Department of Biological Chemistry and Molecular Pharmacology, Harvard Medical School, 240 Longwood Avenue, Boston, Massachusetts 02115, and Department of Chemistry, University of Illinois, 600 South Mathews Avenue, Urbana, Illinois 61801

Received November 8, 2004; Revised Manuscript Received December 6, 2004

ABSTRACT: The aminocoumarin antibiotics clorobiocin and coumermycin A_1 target the B subunit of DNA gyrase by presentation of the 5-methyl-pyrrolyl-2-carboxy ester moiety in the ATP-binding site of the enzyme. The pyrrolyl pharmacophore is derived by a four electron oxidation of a prolyl unit while tethered in phosphopantetheinyl thioester linkage to a peptidyl carrier protein (PCP) subunit. L-Proline is selected and activated as L-prolyl-AMP by adenylation domain enzymes (CloN4 and CouN4) and then installed as the thioester on the holo form of the PCP proteins CloN5 and CouN5. Enzymatic oxidation of the prolyl-*S*-PCP by the flavoprotein dehydrogenase CloN3 can be followed by rapid quench and subsequent electrospray ionization−Fourier transform mass spectrometry analysis of the acyl-*S*-protein substrate/product mixture to establish that a two-electron oxidized pyrrolinyl-*S*-enzyme transiently accumulates on the way to the four-electron oxidized, heteroaromatic pyrrolyl-2-carboxy-*S*-PCP acyl enzyme product.

A wide variety of biologically active natural products contain pyrrole or pyrrole-2-carboxylate moieties. The antifungal agent pyoluteorin (*1*, *2*) has a dichloropyrrole unit, while the red streptomycete metabolite undecylprodigiosin (*3*) has three pyrrole groups, two in tandem array, each made by a distinct path (*4*) (Figure 1A). The aminocoumarin antibiotics clorobiocin and coumermycin A_1 have 5-methylpyrrolyl acyl groups attached to the 3′ hydroxyl of an L-deoxysugar, noviose, which, in turn, is tethered to the aminocoumarin scaffold. The methylpyrrolyl 2-carboxyl moieties are the key pharmacophores (*5*) for interaction with the antibacterial target protein, the B subunit of DNA gyrase (*6*) in the ATP-binding site of this key enzyme in DNA replication. For this reason, we have been interested in the biosynthetic logic of pyrrole-2-carboxylate ring construction and attachment to the aminocoumarin scaffold.

In prior efforts, we established that nonribosomal peptide synthetase (NRPS)[1] enzymatic machinery is operant for the pyoluteorin and prodigiosin pathways (*7*) to activate L-proline and desaturate it while covalently attached in thioester linkage to a carrier protein domain. The gene sequence of the clorobiocin and coumermycin A_1 clusters, determined by Heide and colleagues (*8*−*10*), revealed seven genes, *cloN1*−*7* and *couN1*−*7*, that were involved in pyrrolyl-2-carboxyl construction and attachment to the antibiotic backbone (Figure 1B). Three of the genes, *cou/cloN3*, *-4*, and *-5*, are homologues of orfs in the pyoluteorin and undecylprodigiosin systems. Shown in Figure 1C are proposed roles for the Cou/CloN3, -4, and -5 proteins. The 55-kDa N4 protein has the characteristics of an adenylation (A) domain and is specific for selection of L-proline and activation as L-prolyl-AMP. The 10-kDa N5 protein pair (Cou/Clo) are free-standing peptidyl carrier proteins (PCP), and the 40-kDa CloN3 protein is a flavin-containing dehydrogenase (DH).

Mechanistic studies on the Clo/CouN3, -4, and -5 three-protein systems are complicated by the fact that the products of both N4 and N3 action are covalently bound to the N5 holo-protein by its phosphopantetheinyl arm. Prior studies have relied on base hydrolysis of the protein-bound thioester intermediates to interrogate the soluble amino-acid-derived fragments after release (*11*). In this study, we utilize electrospray ionization−Fourier transform mass spectrometry (ESI−FTMS) to directly detect and characterize prolyl-*S*-N5, measure rates of covalent aminoacyl-*S*-PCP formation, and establish that action by the flavoenzyme CloN3 on the prolyl-*S*-N5 generates the four-electron oxidized pyrrolyl-2-thioester-PCP form of Cou/CloN5 via a two-electron oxidized intermediate.

MATERIALS AND METHODS

Bacterial Strains, Plasmids, Materials, and Instrumentation. Chemically competent *Escherichia coli* TOP10 and BL21 (DE3) cell strains were purchased from Invitrogen. Restriction endonucleases and T4 DNA ligase were pur-

† We gratefully acknowledge the National Institutes of Health Grants GM 20011 (to C.T.W.) and GM 067725 (to N.L.K.).

* To whom correspondence should be addressed: E-mail: christopher_walsh@hms.harvard.edu. Phone: 617-432-1715. Fax: 617-432-0438.

‡ Harvard Medical School.

§ University of Illinois.

[1] Abbreviations: A, adenylation; DH, dehydrogenase; DTT, dithiothreitol; EDTA, ethylenediaminetetraacetic acid; ESI−FTMS, electrospray ionization−Fourier transform mass spectrometry; FAD, flavin adenine dinucleotide disodium salt; HPLC, high-performance liquid chromatography; IPTG, isopropryl-β-thiogalactopyranoside; MALDI−TOF, matrix-assisted laser desorption ionization−time-of-flight; NRPS, nonribosomal peptide synthetase; PCP, peptidyl carrier protein; SDS−PAGE, sodium dodecyl sulfate−polyacrylamide gel electrophoresis; TCA, trichloroacetic acid; TCEP, tris(2-carboxyethylphosphine).

10.1021/bi0476329 CCC: $30.25
Published on Web 02/01/2005

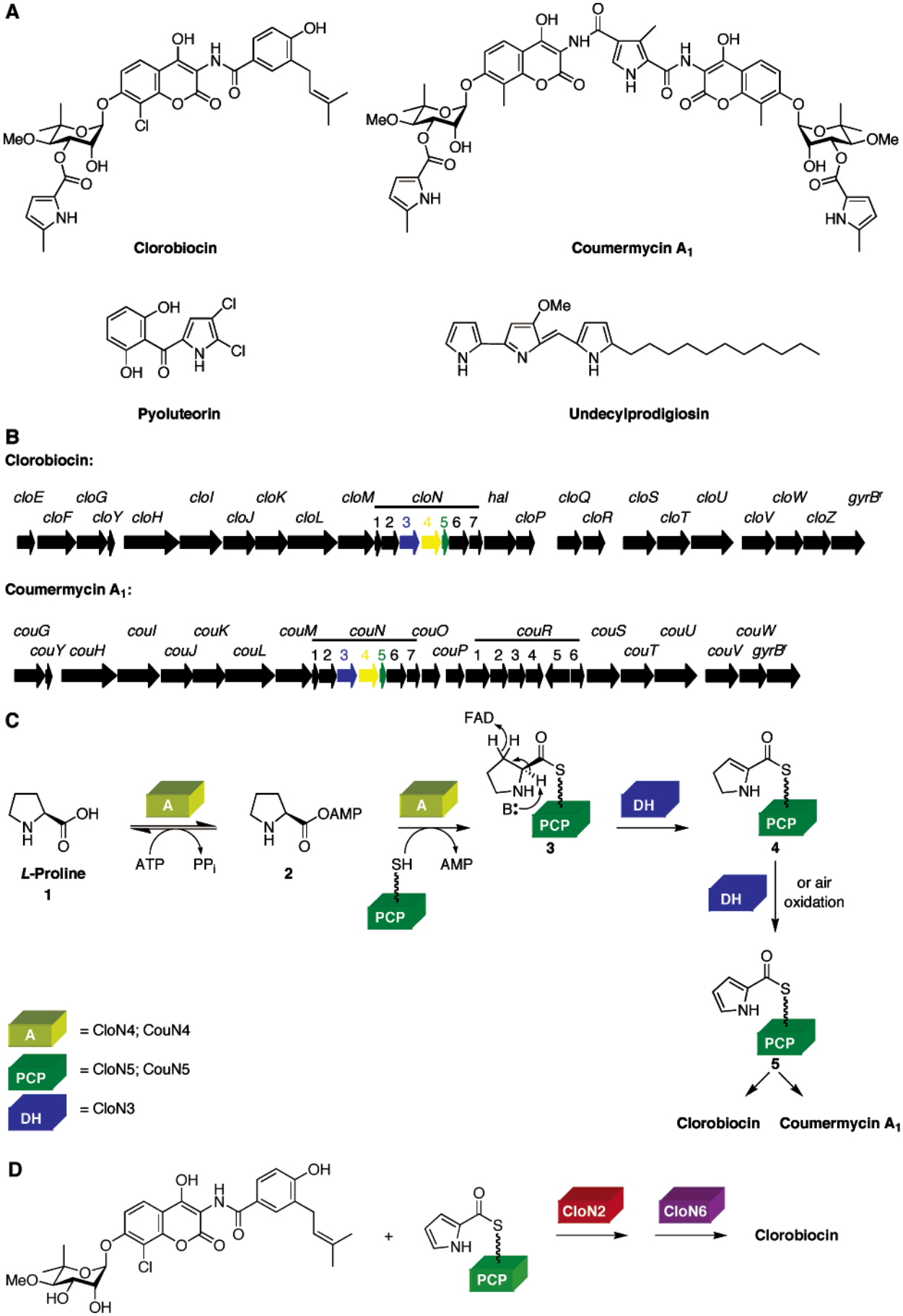

FIGURE 1: (A) Clorobiocin, coumermycin A_1, pyoluteorin, and undecylprodigiosin structures. (B) Clorobiocin and coumermycin A_1 gene clusters. (C) Schematic representation of pyrrol-2-carboxyl-*S*-PCP synthesis from L-proline. (D) Schematic representation of clorobiocin formation from pyrrol-2-carboxyl-*S*-PCP and decorated noviosyl ring.

Table 1: Primers Used for the PCR Amplification of the Clorobiocin and Coumermycin A_1 Genes[a]

gene	5′ primer	3′ primer
cloN3	GTCATAGCTAGCATGGACTTTGACCTCAGCC	CAGTGCCTCGAGTAACCCCATGCTCCTTGCGACAACC
cloN4	GTCATACATATGAGTGATCGGCGCGGCCTCCACGACC	CAGTGCCTCGAGTCACCCTTGAACTTTCTGTGCGCCG
cloN5	GTCATACATATGACGACCCAGACCCGAGAAGAC	CATTGCCTCGAGTCACTTTCGCGACAGGCTCTC
couN4	GTCATACATATGAGTGAAAGGCGCGGCCTCCACGACC	CAGTGCCTCGAGTCACCCTTGAACTTTCTGTGGGCCG
couN5	GTCATACATATGGCAACCCAGACCCGAGAAGAC	CAGTGCGAATTCTTACTTCCGCGACAGGCTCTCATGC

[a] The introduced restriction sites are underlined for each primer. All of the 5′ primers introduced an *Nde*I restriction site except for *cloN3*, which included an *Nhe*I restriction site. All of the 3′ primers included an *Xho*I site except for *couN5*, which introduced an *Eco*RI restriction site.

chased from New England BioLabs. DNA primers for PCR amplification were purchased from Integrated DNA Technologies. *Pfu* Turbo DNA polymerase was purchased from Stratagene. The pET16b, pET24b, and pET28a overexpression vectors were purchased from Novagen. The PPTase Sfp was expressed and purified as previously described (*12*). [^{3}H]-Acetyl-CoA was purchased from Amersham Bioscience. [^{14}C]-L-Proline, [^{3}H]-L-proline, and [^{32}P]PP_i were purchased from Perkin−Elmer. All compounds used for substrate specificity for CloN4 and CouN4 by ATP-[^{32}P]PP_i exchange assays were bought from Aldrich except for the 5-methylpyrrole-2-carboxylic acid that was synthesized by Markus Oberthür in Dan Kahne's laboratory (Princeton University). DNA sequencing and matrix-assisted laser desorption ionization (MALDI) mass spectrometry were performed at the Dana Farber Cancer Institute. High-performance liquid chromatography (HPLC) analysis of enzymatic reaction mixtures was carried out using a Beckman Gold Nouveau System Gold with a Vydac protein and peptide C18 column (250 × 4.6 mm) (for analysis of acylated PCPs) and a Vydac small pore C18 column (250 × 4.6 mm) (for preliminary analysis of the pyrrolyl-*S*-PCP formation by CloN3). ESI−FTMS analyses were performed using a custom-built 8.5 T ESI−FTMS equipped with a front-end quadrupole (*13*).

Preparation of pCloN3-pET24b, pCloN4-pET16b, pCloN5-pET16b, pCouN4-pET16b, and pCouN5-pET28a Overexpression Constructs. The genes encoding CloN3, CloN4, CloN5, CouN4, and CouN5 were PCR-amplified from cosmids provided by Lutz Heide (Pharmaceutical Institute, Tubingen University, Tubingen, Germany). The primers used for the amplification of each gene are listed in Table 1. PCRs were carried out using *Pfu* Turbo DNA polymerase as described by Stratagene. The amplified genes were inserted into the linearized pET24b (*cloN3*), pET16b (*cloN4*, *cloN5*, and *couN4*) and pET28a (*couN5*) vectors via the corresponding *Nde*I/*Xho*I (*cloN4*, *cloN5*, and *couN4*), *Nde*I/*Eco*RI (*couN5*), and *Nhe*I/*Xho*I (*cloN3*) restriction sites. Expression of pCloN3-pET24b, pCloN4-pET16b, pCloN5-pET16b, pCouN4-pET16b, and pCouN5-pET28a was done following transformation into *E. coli* TOP10 competent cells. All expression clones were characterized by DNA sequencing (Dana Farber Cancer Institute) and compared to their corresponding gene sequence from *Streptomyces roseochromogenes* subsp. *oscitans* (*cloN3*, *cloN4*, and *cloN5*) and *S. rishiriensis* (*couN4* and *couN5*) reported by Heide et al. (GenBank entries AAN65232, AAN65233, AAN65234, AAG29789, and AAG29790, respectively).

Overproduction and Purification of CloN3, CloN4, CloN5, CouN4, and CouN5. Purified pCloN3-pET24b, pCloN4-pET16b, pCloN5-pET16b, pCouN4-pET16b, and pCouN5-pET28a plasmids were transformed into *E. coli* BL21 (DE3) competent cells for production and purification. Transformants harboring the pCloN4-pET16b, pCloN5-pET16b, and pCouN4-pET16b constructs were grown in Luria−Bertani (LB) medium (6 × 1 L batches) supplemented with ampicillin (100 μg mL^{-1}), whereas LB broth supplemented with kanamycin (50 μg mL^{-1}) was used for the growth of transformants harboring the pCloN3-pET24b and pCouN5-pET28a constructs. All cells were grown at 25 °C to an OD_{600} of around 0.5. They were subsequently induced by addition of isopropryl-β-thiogalactopyranoside (IPTG) (final concentration of 60 μM) and shaken for an additional 14 h at 25 °C. Cells were harvested by centrifugation (6000 rpm, for 10 min, at 4 °C, Sorvall RC5B centrifuge, SLA-3000 rotor) and resuspended in buffer A [25 mM tris(hydroxymethyl)-aminomethane (Tris)-HCl (pH 8.0), 400 mM NaCl, and 10% (v/v) glycerol]. Resuspended cells were lysed (2 passes at 10 000−15 000 psi, Avestin EmulsiFlex-C5 high-pressure homogenizer), and the cell debris was removed by centrifugation (35 000 rpm, for 30 min, at 4 °C, Beckman L7 Ultracentrifuge, 70Ti rotor). Imidazole (final concentration of 2 mM) was added to the supernatant, which was then incubated with 2 mL of Ni-NTA agarose resin (Qiagen) at 4 °C for 2 h with gentle rocking. The resin was loaded onto a column and washed with 10 mL of buffer A containing 2 mM imidazole and with 10 mL of buffer A containing 5 mM imidazole. The desired proteins were eluted from the column in a stepwise imidazole gradient (5 mL fractions of 20, 40, 60, 200, and 500 mM imidazole). Fractions containing the pure target proteins [as determined by sodium dodecyl sulfate−polyacrylamide gel electrophoresis (SDS−PAGE)] were combined and dialyzed overnight at 4 °C against 1 L of buffer B [50 mM Tris-HCl (pH 8.0 adjusted at room temperature), 100 mM NaCl, 1 mM ethylenediaminetetraacetic acid (EDTA), 1 mM dithiothreitol (DTT), and 10% (v/v) glycerol]. A second dialysis was carried out for 4 h at 4 °C in 1 L of buffer C [50 mM Tris-HCl (pH 8.0 adjusted at room temperature), 100 mM NaCl, 1 mM DTT, and 10% (v/v) glycerol]. Proteins were concentrated using either Amicon Ultra PL-10 or Amicon Ultra PL-5 for either CloN3, CloN4, and CouN4 or CloN5 and CouN5, respectively. Proteins were flash-frozen in liquid nitrogen and stored at −80 °C. Protein concentrations were determined using the Bradford assay (Bio-Rad).

Substrate Specificity by ATP-[^{32}P]PP_i Exchange Assays for Aminoacyl-AMP Formation. To determine substrate specificity, ATP-[^{32}P]PP_i reactions (100 μL) containing Tris-HCl (pH 7.5) (75 mM), $MgCl_2$ (10 mM), tris(2-carboxyethylphosphine) (TCEP) (pH 7.0) (5 mM), ATP (5 mM), amino acid substrate (5 mM), and 1 mM [^{32}P]PP_i (55 Ci/mM) were performed at 25 °C. The reactions were started by addition of CloN4 or CouN4 at a final concentration of 1 μM. Reactions were incubated for 1.5 h before quenching with charcoal suspensions (500 μL) [1.6% (w/v) activated char-

coal, 4.5% (w/v) tetrasodium pyrophosphate, and 3.5% (v/v) perchloric acid in H_2O]. Centrifugation was applied to provide the charcoal pellet. The pellet was then washed twice with the wash solution (500 μL) [4.5% (w/v) tetrasodium pyrophosphate and 3.5% (v/v) perchloric acid in H_2O], resuspended in H_2O (500 μL), and submitted for liquid scintillation counting (Beckman LS6500, Beckman Coulter, Fullerton, CA). For the determination of K_m and k_{cat} for the L-proline activation, reactions (100 μL) containing Tris-HCl (pH 7.5) (75 mM), $MgCl_2$ (10 mM), TCEP (pH 7.0) (5 mM), ATP (5 mM), and 1 mM [^{32}P]PP_i (55 Ci/mM, from Perkin−Elmer) and varying concentrations of L-proline (0.05, 0.1, 0.25, 0.5, 1, 1.75, 2,5, 5, 10, and 17 mM) were performed at 25 °C. The reactions were initiated by addition of CloN4 (1 μM) or CouN4 (1 μM) and were stopped after 25 min. The experiments were carried out 3 times for each substrate concentration.

Holo-PCP Aminoacylation by Tricholoracetic Acid (TCA) Precipitation Assays. Incorporation of [^{14}C]-L-proline and [^{3}H]-L-proline into holo-PCPs was monitored by TCA precipitation assays. A time course for the aminoacylation of the holo-PCPs by each of the L-prolyl-AMP ligases involved a reaction mixture (600 μL) containing Tris-HCl (pH 7.5) (75 mM), $MgCl_2$ (10 mM), TCEP (pH 7.0) (5 mM), ATP (5 mM), radiolabeled L-proline (0.5 mM), L-prolyl-AMP ligase (CloN4 or CouN4) (1 μM), and holo-PCP (2.5 μM) [CloN5 or CouN5 obtained by priming of apo-PCP (25 μM) using Sfp (1 μM), CoA (50 μM), Tris-HCl (pH 7.5) (75 mM), $MgCl_2$ (10 mM), and TCEP (pH 7.0) (5 mM)]. Samples of 50 μL were removed at 2, 5, 10, 15, 30, 45, and 60 min and added to 10% TCA (200 μL). Protein was pelleted by centrifugation, washed with 10% TCA, washed twice with H_2O (1 mL), and resuspended in 88% formic acid. The radiolabeled product was counted by liquid scintillation counting.

MALDI−Time-of-Flight (TOF) Mass Spectrometry. To determine the mass of apo-proteins and holo-PCP domains, initial mass spectrometry analyses on purified proteins (Zip Tip C4, Millipore) were performed with a linear MALDI−TOF mass spectrometer. Samples were prepared by using α-sinapinic acid (10 mg mL^{-1} in 60% acetonitrile/H_2O) as the matrix. Cal3 (MH^+ = 5734.51, 12 361.96, and 16 952.27 Da) was used for calibration of the instrument, which was performed before each experiment.

HPLC Analysis of Purified Apo-, Holo-, and Acylated-PCPs. Apo-, holo-, and acylated-PCPs (CloN5 and CouN5) were separated by HPLC (Beckman System Gold) with a Vydac protein and peptide C18 column (250 × 4.6 mm) at a flow rate of 1 mL min^{-1}. The acylation of the holo-PCP was performed using Tris-HCl (pH 7.5) (75 mM), $MgCl_2$ (10 mM), TCEP (pH 7.0) (5 mM), ATP (5 mM), holo-PCP (8 μM), CouN4 or CloN4 (1 μM), and substrate (0.25 mM). The HPLC gradient was a 20−60% acetonitrile, 0.1% TFA gradient over 20 min. Product elution was monitored at 220 nm.

Preparation of the Samples for Analysis by ESI−FTMS. Assay mixtures (typically 100−200 μL) were acidified 1:1 in 10% formic acid and desalted by purifying the proteins of interest. An HPLC equipped with a Jupiter 5m C4 300 Å (150 × 4.6 mm 5m) Phenomenex column was used for desalting. The gradient was a 10−90% acetonitrile, 0.1% TFA gradient over 30 min at a flow rate of 1 mL min^{-1}. The proteins eluted at the following times: Sfp, 16.7 min; apo-CloN5, 21.7 min; holo-CloN5, 20.2 min; L-prolyl-*S*-CloN5, 19.8 min; CloN5 (two-electron oxidation product), 19.8 min; pyrrolyl-*S*-CloN5, 20.4 min; and CloN3, 21.4 min. Each peak that eluted from the HPLC as monitored at 220 and 280 nm was collected as a separate fraction or a single fraction from 19.6 to 20.6 min. Once collected, the fractions were frozen at −80 °C before placing them in a lyophilizer. Once the solution had been lyophilized, the samples were stored at −80 °C until ESI−FTMS analysis. For ESI−FTMS analysis, the samples were redissolved in methanol/water (1:1 containing 2% formic acid) and analyzed using a custom-built 8.5 T quadrupole-FTMS hybrid mass spectrometer operating at 8.5 T (*13*). The quadrupole allows for the isolation and signal enhancement of a specific region of the spectrum. The resulting masses of the proteins were calculated by importing the data into THRASH, and the resulting masses were confirmed manually or by a new match in MIDAS data analysis software (*14*). All masses obtained by ESI−FTMS throughout this paper are given as monoisotopic values. In all of the mass spectra of both CloN5 and CouN5, an additional mass of +178 Da is observed. This mass shift can be due to the addition of a noncovalent pyrophosphate (*15*), or it can be a glycosylation of His-tagged proteins during expression (*16*). MS/MS of the +178-Da species by collisional activation resulted in fragment ions containing the +178 Da on the C-terminal end of the protein, consistent with a covalent modification in the His-tag region of the protein.

Partial Localization of the Modifications on CloN5 and CouN5 by MS/MS. The covalent modifications on CloN5 and CouN5 were localized using MS/MS, where the fragments were generated using collissionally activated dissociation (CAD) following the mass selection of the mass range of interest in the front-end quadrupole. THRASH and/or a new match in MIDAS data analysis software were used to generate the monoisotopic masses for the fragments. For the ^{13}C,^{15}N-depleted samples, the fragment list was generated determining the charge state from the isotopes and multiplying this charge state with the observed mass. After the monoisotopic masses were obtained, the list of fragments was incorporated into ProSight PTM (single-protein mode) (*17*) to localize the modifications.

Preparation of ^{13}C,^{15}N-Depleted CloN5 and CouN5. An overnight culture of a BL21 (DE3) overexpression strain containing a plasmid encoding CloN5 or CouN5, in LB medium (5 mL) supplemented with ampicillin (CloN5, 50 μg mL^{-1}) or kanamycin (CouN5, 20 μg mL^{-1}), was spun down in a clinical centrifuge, and the supernatant was discarded. The cell pellet was washed 3 times with wash buffer (5 mL, 3 g of KH_2PO_4, 6 g of Na_2HPO_4, and 0.5 g of NaCl L^{-1} at pH 7.4), resuspended in wash buffer (2 mL), and added to modified M9 minimal media (300 mL) (pH 7.4) containing 1 g of KH_2PO_4, 2 g of Na_2HPO_4, 0.2 g of NaCl, 0.8 mL of 40% $(^{14}NH_4)_2SO_4$, 0.50 g of ^{13}C-depleted glucose, 0.2 mg of $FeCl_3$, 20 μg of thiamin, 400 μL of 1 M $MgSO_4$, 20 μL of 1 M $CaCl_2$, 50 μg mL^{-1} of ampicillin or 20 μg mL^{-1} of kanamycin, and 300 μL of a trace-element solution containing 0.55 g of $CaCl_2$, 0.17 g of $ZnCl_2$, 0.043 g of $CuCl_2 \cdot H_2O$, 0.06 g of $CoCl_2 \cdot 6H_2O$, and 0.06 g of $Na_2MoO_4 \cdot 2H_2O$ L^{-1} at pH 7.4. The cells were induced at OD_{595} = 0.8 (after ∼5−7 h) by addition of IPTG (50 mg) and

grown with agitation at 37 °C for an additional 8 h. The cell pellet containing overexpressed ^{13}C,^{15}N-depleted CloN5 or CouN5 was frozen at −20 °C until use. The proteins were then purified by Nickel-affinity chromatography (NTA-superflow resin by Qiagen) and buffer-exchanged using a PD10 column (Amersham) equilibrated with 50 mM Tris-HCl (pH 7.6). The samples were stored at −80 °C as 5% (v/v) glycerol stocks until use.

Detection of the ^{13}C,^{15}N-Depleted Pyrrolyl-S-PCP by ESI−FTMS. The ^{13}C,^{15}N-depleted pyrrolyl-*S*-CloN5 was prepared by the addition of CloN3 (2.5 μM) and flavin adenine dinucleotide disodium salt (FAD) (100 μM) to ^{13}C,^{15}N-depleted L-prolyl-*S*-CloN5 (20 μM) (200 μL reaction volume), which was prepared as described above for the formation of the nondepleted CloN5. The reaction was quenched at 5 min by the addition of 10% formic acid (200 μL). Detection of the pyrrolyl-*S*-CloN5 was achieved by collecting the HPLC fraction at 20.4 min and analyzing it by ESI−FTMS as described above. For the detection of the ^{13}C,^{15}N-depleted pyrrolyl-*S*-CouN5, identical conditions were used except that we collected a fraction from 19.7 to 20.7 min.

Rapid Quench to Detect the 2-Da Oxidation of ^{13}C,^{15}N-Depleted L-Prolyl-S-CloN5. L-Proline acylated CloN5 (acylation was confirmed by HPLC) (100 μL of 26.5 μM) was reacted with CloN3 (100 μL of 66.4 μM) and FAD (100 μM) in a 1:1-dependent reaction. The reaction was mixed and quenched with 10% formic acid using a rapid-quench apparatus (Kintek Chemical Fast Quench) at various time points in the millisecond to minute time range. Each time point was HPLC-purified, and the fraction from 19.6 to 20.6 min was analyzed by ESI−FTMS. The rapid-quench studies were performed at 25 or 30 °C.

Loading and Oxidation of 3,4-Dehydro-L-proline. CloN5 (500 μL of 10 μM) was pantetheinylated and loaded with 3,4-dehydro-L-proline as described. Once we observed a new peak at 19.8 min (HPLC conditions as described in the ESI−FTMS section) for the loaded 3,4-dehydro-L-prolyl-*S*-CloN5 by HPLC, we added FAD (100 μM) and CloN3 (3 μM) to 200 μL of this solution and allowed it to incubate at room temperature for 35 min before quenching with 10% formic acid (200 μL). The resulting solution was analyzed by HPLC, and a new peak at 20.4 min appeared. This peak comigrated with the pyrrolyl-*S*-CloN5, and the mass was confirmed by ESI−FTMS.

Relative Rates of Oxidation of the 3,4-Dehydro-L-proline. CloN5 (1400 μL of 10 μM) was pantetheinylated using Sfp (1 μM), $MgCl_2$ (8 mM), and CoA (200 μM). After 1 h, ATP (4 mM) and CloN4 (0.5 μM) were added before the mixture was split in two. 3,4-Dehydro-L-proline or proline (5 mM) were added to separate the assay mixtures. After 20 min, acylation was confirmed by HPLC. Once the acylation was confirmed, FAD (100 μM) and CloN3 (0.3 μM) were added and the conversion was monitored over 146 min by quenching 200 μL of the reaction mixture with 10% formic acid (200 μL) before HPLC analysis. To determine the relative rate of oxidation of L-prolyl-*S*-CloN5 versus 3,4-dehydro-L-prolyl-*S*-CloN5, the 19.8 and 20.4 peaks were integrated and plotted in Sigmaplot.

Relative Rates of Oxidation by CloN3 of Acetylated CloN5 and CouN5. A total of 250 μL of 10 μM of L-prolyl-*S*-CloN5 and 250 μL of 10 μM of L-prolyl-*S*-CouN5 were prepared as described above. Upon addition of CloN3 (final concentration of 1 μM, 250 pmol total) and FAD (100 μM), 50 μL aliquots of the reaction were quenched (1:1) over time with 10% formic acid and analyzed by HPLC. The resulting intensities at 220 nm for the L-prolyl-*S*-PCP and pyrrolyl-*S*-PCP were integrated and imported into Sigmaplot, and the initial rates were calculated. The rates determined for the formation of pyrrolyl-*S*-CloN5 and pyrrolyl-*S*-CouN5 are 12.5 and 2.9 pmol min^{-1}, respectively.

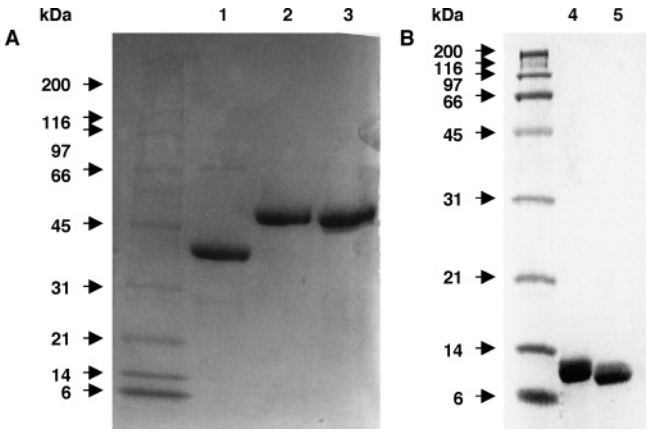

FIGURE 2: (A) Tris-HCl (4−15%) SDS−PAGE of purified CloN3 (lane 1), CloN4 (lane 2), and CouN4 (lane 3) detected by Coomassie blue staining. (B) Tris-HCl (15%) SDS−PAGE of purified CloN5 (lane 4) and CouN5 (lane 5) detected by Coomassie blue staining.

Table 2: MALDI−TOF Mass Analysis of Purified Apo- and Holo-proteins

protein	calculated $[M + H]^+$	observed $[M + H]^+$
CloN3	40 416	40 470
CloN4[a]	56 089	56 077
apo-CloN5[a]	12 319 (12 188)	12 346 (12 163)
holo-CloN5[a]	12 659 (12 528)	12 696 (12 516)
acetyl-*S*-CloN5[a]	12 701 (12 570)	12 737 (12 556)
L-prolyl-*S*-CloN5[a]	12 756 (12 625)	12 780 (12 613)
trans−4-hydroxy-L-prolyl-*S*-CloN5[a]	12 772 (12 641)	12 779 (12 630)
3,4-dehydro-L-prolyl-*S*-CloN5[a]	12 754 (12 623)	12 790 (12 611)
CouN4	55 819	54 222
apo-CouN5[a]	11 885 (11 754)	11 936 (11 726)
holo-CouN5[a]	12 225 (12,094)	12 227 (12 070)
acetyl-*S*-CouN5[a]	12 267 (12 136)	12 288 (12 123)
L-prolyl-*S*-CouN5[a]	12 322 (12 291)	12 326 (12 173)
trans−4-hydroxy-L-prolyl-*S*-CouN5[a]	12 338 (12 207)	12 264 (12 082)
3,4-dehydro-L-prolyl-*S*-CouN5[a]	12 320 (12 289)	12 325 (12 271)

[a] Mass in parentheses is missing the first methionine.

RESULTS

Heterologous Expression and Purification of the A (CloN4 and CouN4), PCP (CloN5 and CouN5), and DH (CloN3) Domain Proteins of Clorobiocin and Coumermycin A_1. To evaluate the proposed roles of the N3, -4, and -5 proteins of the related clorobiocin (Clo) and coumermycin (Cou) in their respective biosynthetic pathways, we started with heterologous expression of the proteins in *E. coli* as His-tagged constructs. As shown in Figure 2, the CouN4 and CloN4 proteins and the CloN3 protein were obtained in soluble form after metal-affinity chromatography, as well as the low molecular weight CouN5 and CloN5 proteins, the proposed substrates for N4 adenylations. MALDI−TOF analysis (Table 2) gave molecular weights consistent with the predicted molecular weights.

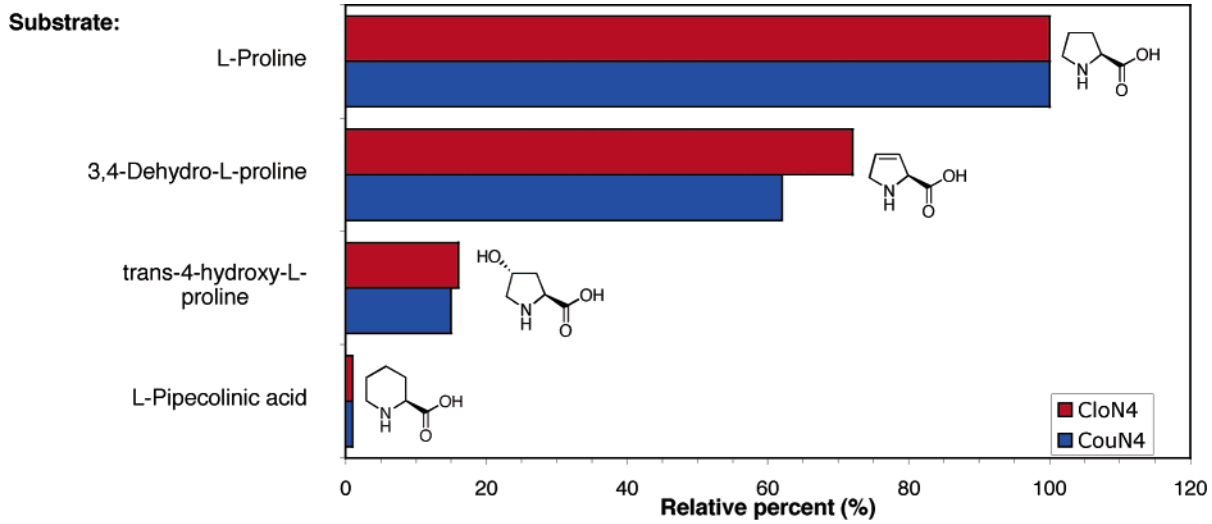

FIGURE 3: Relative substrate specificity determined by ATP-[^{32}P]PP$_i$ exchange assay catalyzed by CloN4 (red) and CouN4 (blue). Data are representative of 25 min end-point assays.

Table 3: Kinetic Parameters of the ATP-[^{32}P]PP$_i$ Exchange Assay for CloN4 and CouN4

modification	enzyme	K_m (mM)	k_{cat} (min^{-1})
L-prolyl-AMP formation	CloN4	0.53 ± 0.08	13.1 ± 0.5
	CouN4	1.16 ± 0.08	2.5 ± 0.1

Characterization of A Domains CloN4 and CouN4. The CloN4 and CouN4 proteins are predicted to behave as free-standing A domains, with two half-reactions. The first is ATP-dependent activation of L-proline as L-prolyl-AMP to activate the carboxyl group. The second half-reaction is transfer of the activated aminoacyl moiety (L-prolyl) to the PCP, the cognate N5 protein. The first half-reaction is typically assayed by amino-acid-dependent exchange of radioactivity from ^{32}PP$_i$ into ATP, and Figure 3 validates this expectation for L-prolyl-AMP formation by both CloN4 and CouN4. A variety of proline analogues were assayed, and only the 3,4-dehydro-L-proline and the *trans*-4-hydroxy-L-proline sustained the PP$_i$−ATP exchange. The six-ring imino acid analogue, L-pipecolinic acid, was a weak substrate. The 13 other compounds [(*R*)-(+)- and (*S*)-(−)-tetrahydro-2-furoic acid, 2-furoic acid, (*R*)-(+)- and (*S*)-(−)-2-pyrrolidone-5-carboxylic acid, pyrrole-2-carboxylic acid, 5-methyl-2-thiophene carboxylic acid, *N*-methyl-L-proline, 1-methyl-2-pyrrole carboxylic acid, D-pipecolinic acid, D-proline, 2-thiophene carboxylic acid, and 3-methyl-2-thiophene carboxylic acid] that were assayed for substrate−AMP formation by ATP-[^{32}P]PP$_i$ exchange reactions were found to not be accepted by CloN4 and CouN4. On the basis of the criterion of catalytic efficiency (k_{cat}/K_m), CloN4 is about a 10-fold better catalyst than CouN4 for this first half-reaction (Table 3).

Characterization of PCP Domains CloN5 and CouN5. The second half-reaction of the A domain activity of CloN4 and CouN4 involves recognition of the PCP partner proteins, CloN5 and CouN5, and transfer of the activated L-prolyl moiety to the PCP. For this to occur, the PCP proteins must be post-translationally modified, on a specific serine residue, with a phosphopantetheinyl group derived from CoASH. As shown in Table 2 and Figure 4, both CloN5 and CouN5 are overproduced in the expected apo forms in *E. coli*, because *E. coli* cells do not have phosphopantetheinyl transferases that recognize apo forms of PCP domains (*18*). We have previously characterized the Sfp phosphopantetheinyl transferase from surfactin-producing Bacilli (*19*, *20*) as a promiscuous phosphopantetheinyl transferase, and Sfp serves effectively to convert apo forms of CloN5 and CouN5 to the phosphopantetheinylated forms, as measured both by the gain of 340 Da by MALDI−TOF analysis (Table 2) and by the clear difference in HPLC mobility (lines A and B, G and H of Figure 4). The acetylated holo forms of CloN5 and CouN5 also have distinct HPLC mobility as noted in lines C and I of Figure 4.

Therefore, quantitative generation of the holo forms of CloN5 and CouN5 was achieved by preincubation with CoASH and Sfp as a prelude to the assay of the second half-reaction of CloN4 and CouN4. L-Prolyl transfer to generate the L-prolyl-*S*-CloN4 or L-prolyl-*S*-CouN4 could be confirmed by several routes, including covalent attachment of radiolabeled L-proline (data not shown). Lines B and D of Figure 4 show a substantial HPLC shift because holo-CloN5 is quantitatively converted to L-prolyl-*S*-CloN5 in the presence of L-proline, ATP, and CloN4. An equivalent shift is seen in lines H and J with holo-CouN5 conversion to L-prolyl-*S*-CouN5. The second half-reaction also proceeds with the proline analogues of Figure 3. Lines E and F show the diagnostic HPLC traces for *trans*-4-hydroxy-L-prolyl-*S*-CloN5 and 3,4-dehydro-L-prolyl-*S*-CloN5, while line K shows the corresponding HPLC trace for 3,4-dehydro-L-prolyl-*S*-CouN5. In contrary to the pyoluteorin and undecylprodigiosin systems where PltF and Orf11 only work with their corresponding PCP, each N4 protein will transfer the activated prolyl moiety to both of the holo-CloN5 and holo-CouN5 proteins (data not shown), consistent with high homology and equivalent function in the two antibiotic biosynthetic pathways.

Direct Observation of the Pantetheinoylation and Acylation of CloN5 and CouN5 by ESI−FTMS. An additional route for direct detection of the aminoacyl-*S*-PCP proteins was ESI−FTMS analysis. The low molecular weight (~12 kDa) of the free-standing PCP proteins, CloN5 and CouN5, facilitates direct detection of the intact protein. The prolyl-thioester linkage to the pantetheinyl arm of the PCPs is stable in acid used for quenching and storage of the covalent

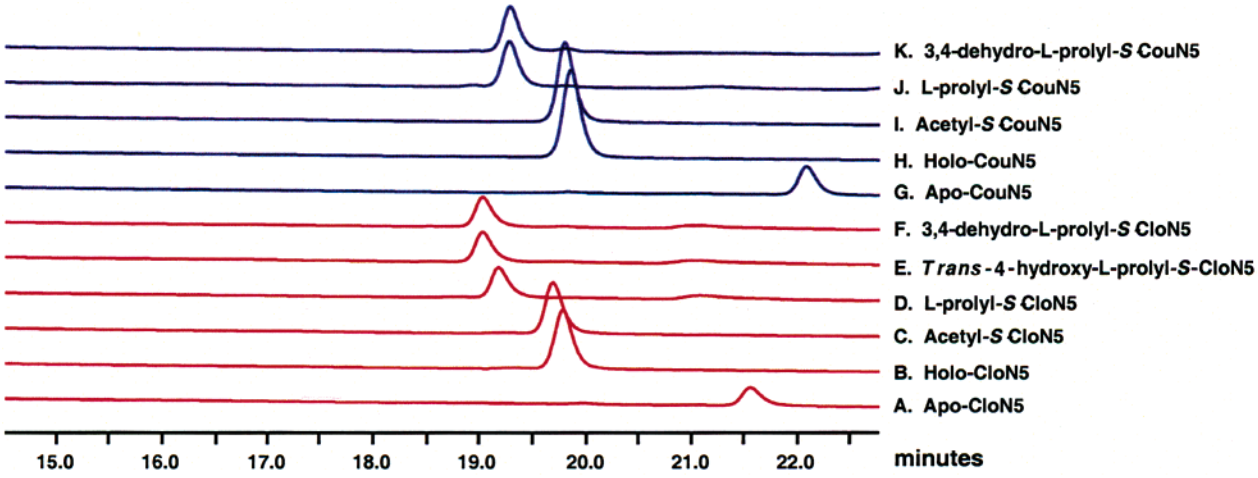

FIGURE 4: HPLC analysis of various PCPs. (A) Apo-CloN5 as purified from *E. coli*. (B) Holo-CloN5 resulting from Sfp modification of the apo-CloN5 with free CoA. (C) Acetyl-*S*-CloN5 obtained by Sfp modification of the apo-CloN5 with acetyl-CoA. (D) L-Prolyl-*S*-CloN5 obtained by Sfp modification of the holo-CloN5 with L-proline and CloN4. (E) *Trans*-4-hydroxy-L-prolyl-*S*-CloN5 obtained by Sfp modification of the holo-CloN5 with *trans*-4-hydroxy-L-proline and CloN4. (F) 3,4-Dehydro-L-prolyl-*S*-CloN5 obtained by Sfp modification of the holo-CloN5 with 3,4-dehydro-L-proline and CloN4. (G) Apo-CouN5 as purified from *E. coli*. (H) Holo-CouN5 resulting from Sfp modification of the apo-CloN5 with free CoA. (I) Acetyl-*S*-CouN5 obtained by Sfp modification of the apo-CouN5 with acetyl-CoA. (J) L-Prolyl-*S*-CouN5 obtained by Sfp modification of the holo-CouN5 with L-proline and CouN4. (K) 3,4-Dehydro-L-prolyl-*S*-CouN5 obtained by Sfp modification of the holo-CouN5 with 3,4-dehydro-L-proline and CouN4.

intermediates until MS analysis. As shown in A and B of Figure 5, the apo form of CloN5 gives the anticipated molecular weight of 12 180, in excellent agreement with the predicted value. The holo form of CloN5 correspondingly shows the +340 Da increase (Figure 5C), confirming that the species with altered mobility in line B of Figure 4 is indeed the pantetheinylated holo form with the terminal thiol moiety that is the nucleophile for prolylation. Figure 5D shows the further increase of 97 mass units for the addition of the prolyl group to the holo form as L-prolyl-*S*-CloN5 is detected. The ability to detect L-prolyl-*S*-CloN5 by ESI−FTMS is a necessary precondition for the experiments detailed below with CloN3.

Characterization of DH Domain CloN3. On expression of the putative L-prolyl-*S*-PCP oxidases, CloN3 and CouN3, in *E. coli*, CloN3 gave soluble protein that was yellow, because of bound FAD (as determined by HPLC), consistent with our expectation and experience from the pyoluteorin and undecylprodigiosin systems (*7*). CouN3 was not immediately tractable, and because CloN3 oxidizes the covalently tethered prolyl thioester on both CloN5 and CouN5 scaffolds, we pressed ahead with CloN3. CloN3 was incompletely loaded with FAD after the Ni-NTA column isolation step and was assayed with excess FAD added.

Oxidation of L-Prolyl-S-PCP to Pyrrolyl-S-PCP. The expectation for CloN3 is that it acts on L-prolyl-*S*-CloN5 to oxidize it to pyrrolyl-*S*-CloN5. Then, the planar heteroaromatic pyrrolyl-2-thioester should be a substrate for CloN2 (*21*), proposed to transfer the pyrrolyl moiety to the 3′-OH of the noviosyl moiety in the next to last step of clorobiocin assembly (Figure 1D) (*21*). To that end, we wanted to assay for oxidation of the PCP-bound prolyl group by CloN3 to the −2-Da (dehydro-L-prolyl) and then the −4-Da (pyrrolyl) acyl-*S*-PCP. In initial assays, release of the thioester after CloN3 action confirmed (by HPLC, data not shown) that the prolyl moiety was converted to the pyrrolyl-2-carboxy. Similar cleavage assays starting with [^{14}C]-L-prolyl-*S*-PCP confirmed (by radiolabeled TLC, data not shown) the formation of the pyrrolyl moiety.

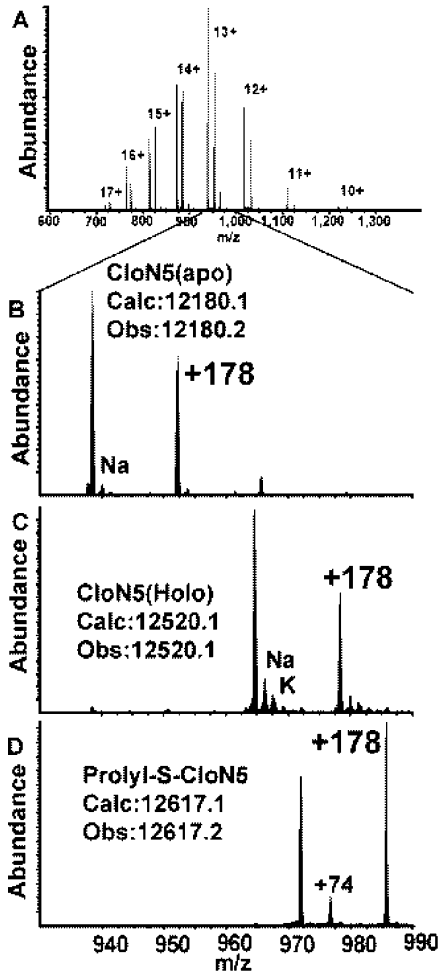

FIGURE 5: Direct observation of pantetheinylation and acylation of proline by ESI−FTMS. (A) Whole mass spectrum obtained with apo-CloN5. (B) Enlargement of the mass spectrum of apo-CloN5 from 930 to 990 mass to the charge (*m*/*z*) region. (C) Mass spectrum of CloN5 following treatment with Sfp (a PPTase) and CoA to generate holo-CloN5. (D) Mass spectrum of L-prolyl-*S*-CloN5.

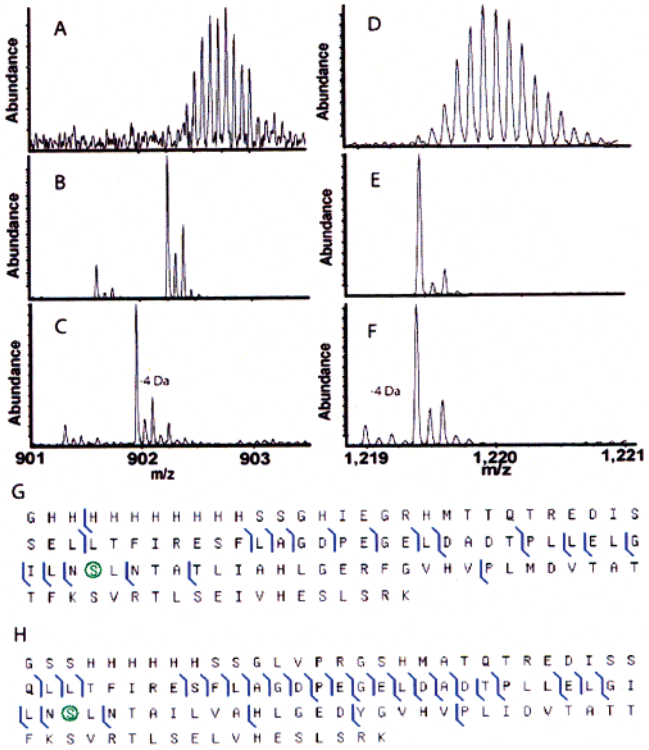

FIGURE 6: Direct observation of the pyrrolyl-*S*-CloN5 and pyrrolyl-*S*-CouN5 using $^{13}C,^{15}N$-depleted protein. (A) Mass spectrum of the nondepleted L-prolyl-*S*-CloN5. (B) Mass spectrum of $^{13}C,^{15}N$-depleted L-prolyl-*S*-CloN5. (C) Mass spectrum following the treatment of $^{13}C,^{15}N$-depleted L-prolyl-*S*-CloN5 with FAD and CloN3. (D) Mass spectrum of the nondepleted L-prolyl-*S*-CouN5. (E) Mass spectrum of $^{13}C,^{15}N$-depleted L-prolyl-*S*-CouN5. (F) Mass spectrum following the treatment of $^{13}C,^{15}N$-depleted L-prolyl-*S*-CouN5 with FAD and CloN3. (G) Localization of the oxidation product by MS/MS. The serine with the circle indicates the increase in mass for the pyrrolyl-*S*-CloN5 when compared to apo-CloN5, an increase of 433.1 Da. (H) Localization of the oxidation product by MS/MS. The serine with the circle indicates the increase in mass for the pyrrolyl-*S*-CouN5 when compared to apo-CouN5, an increase of 433.1 Da.

Because of the isotopic distribution envelope even in a small protein, we anticipated it would be difficult to unambiguously observe a 0.016% (loss of 2-Da) or 0.032% (4-Da) difference in mass of the intact 12-kDa protein. This would be of particular relevance in kinetic analyses, where there is a low percentage of conversion to the oxidized species (−4 Da) or mixtures of unoxidized, partially oxidized (−2-Da) and fully oxidized (−4-Da) species. Therefore, to reduce the width of the isotope envelope, $^{13}C,^{15}N$-depleted CloN5 and CouN5 were prepared. This allows for the unambiguous identification of the loss of 2 and 4 Da, (parts A and B of Figure 6) even when they are mixtures or when there are low conversions, because we can directly "see" the monoisotopic peak.

When L-prolyl-*S*-CloN5 was treated with CloN3, a new peak at 20.4 min appeared and the L-prolyl-*S*-CloN5 eluting at 19.8 min decreased. ESI−FTMS analysis of this new fraction indicated that it was the 4-Da oxidized product, pyrrolyl-*S*-CloN5 (Figure 6C). In a similar fashion, L-prolyl-*S*-CouN5 could be oxidized by CloN3 to the pyrrolyl-*S*-CouN5 (Figure 6F) albeit at ~25% of the rate when compared to L-prolyl-*S*-CloN5 (see the Materials and Methods). The pyrrolyl group could be localized by MS/MS (parts G and H of Figure 6) to a region of the protein that includes

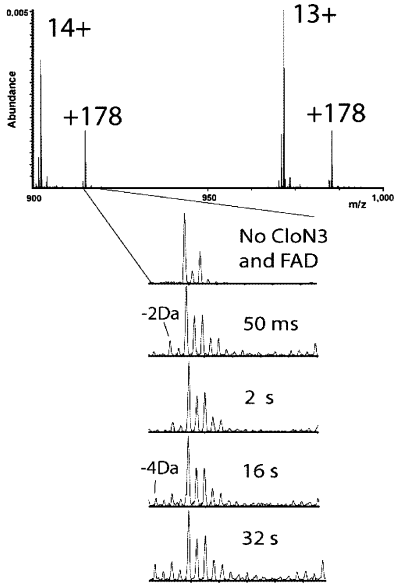

FIGURE 7: Direct observation of the 2-Da oxidation intermediate from a single oxidation of $^{13}C,^{15}N$-depleted L-prolyl-*S*-CloN5 using rapid quench. (Top) Mass spectral region of 900−1000 *m/z* showing the 14+ and 13+ charge states. The enlargement shows the time-dependent increase of the −2-Da oxidation intermediate and the −4-Da oxidation product, the $^{13}C,^{15}N$-depleted pyrrolyl-*S*-CloN5.

the serine bearing the acylated pantetheinyl functionality. In these experiments, the anticipated 2-Da oxidized intermediate was not observed. Because it was possible that the second oxidation was faster than the first oxidation, rapid-quench methods were used to search for the anticipated stepwise two-electron (−2-Da) oxidation.

Excess CloN3 and FAD Was Rapidly Mixed with L-Prolyl-S-CloN5, Quenched at Different Time Points, and Desalted, and the HPLC Fraction from 19.6 to 20.7 min Was Analyzed by ESI−FTMS. As shown in Figure 7, the −2-Da species was detected at 50 ms. Over time, the −2-Da species is converted to the −4-Da pyrrolyl-*S*-CloN5. The 2-Da oxidation intermediate was observed transiently but only when excess CloN3 is used. Because we do not see a large build-up of the 2-Da oxidized intermediate, the dehydro-L-prolyl/pyrrolinyl-*S*-PCP is probably not released from the active site of CloN3 before it is converted in a second two-electron oxidation step to the pyrrolyl-*S*-CloN5.

C2−C3 versus C2−N Oxidation. Given that CloN4 activates 3,4-dehydro-L-proline, we analyzed if this two-electron oxidized (−2-Da) form of a L-prolyl-*S*-CloN5 would be acted on by CloN3 to yield the heteroaromatic pyrrolyl-*S*-PCP. Indeed, upon incubation of 3,4-dehydro-L-prolyl-*S*-CloN5 with FAD and CloN3, the peak eluting by HPLC at 19.8 was converted to 20.4 min. This is the identical elution time as the pyrrolyl-*S*-CloN5 obtained from the oxidation of L-prolyl-*S*-CloN5. The rate of conversion from the 3,4-dehydro-L-prolyl-*S*-CloN5 to the pyrrolyl-*S*-CloN5 is 8.3 times faster than the corresponding proline analogue, establishing that it could be a kinetically competent intermediate on the way from the prolyl-*S*-PCP starting substrate (Figure 8).

DISCUSSION

The 5-methylpyrrolyl-2-carboxyl moiety found in clorobiocin and coumermycin A_1 serves as a planar, heteroaro-

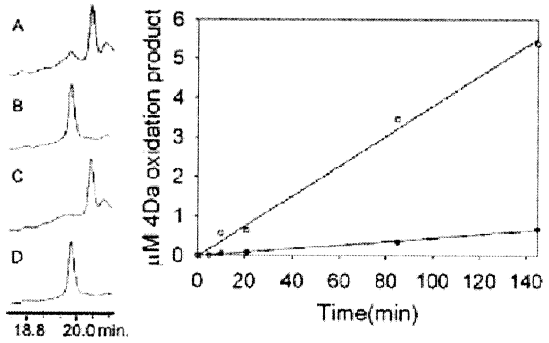

FIGURE 8: HPLC analysis for the oxidation of 3,4-dehydro-L-prolyl-*S*-CloN5 to pyrrolyl-*S*-CloN5 upon treatment with FAD and CloN3. (A) Oxidized L-prolyl-*S*-CloN5. (B) L-Prolyl-*S*-CloN5. (C) Oxidized 3,4-dehydro-L-prolyl-*S*-CloN5. (D) 3,4-Dehydro-L-prolyl-*S*-CloN5. (E) Relative rates of conversion of L-prolyl-*S*-CloN5 and 3,4-dehydro-L-prolyl-*S*-CloN5 to pyrrolyl-*S*-CloN5.

matic functional group with hydrogen-bonding properties that make it a useful pharmacophore in many classes of small molecules that interact with biological targets. The dichloropyrrolyl moiety in pyoluteorin and the first of the three pyrrole groups in prodigiosins derive biosynthetically from the same pyrrole-2-carboxylate skeleton. The five-membered heteroaromatic pyrrole, similar to the five-membered oxazole (from Ser) and thiazole (from Cys) rings in small-molecule natural products (*22*), derive biosynthetically from proteinogenic amino acids that have been diverted down secondary metabolite pathways (*23*).

While there are several enzymatic routes to pyrroles (three different ones for each of the three pyrrole rings in undecylprodigiosin) (*3*, *7*), L-proline is the unsurprising precursor of the pyrrole ring for the aminocoumarin antibiotics. However, the route for diversion of a fraction of the producer cell pool of L-proline to pyrrole-2-carboxylate is emblematic of a general strategy for controlled flux of primary amino acids into specialized products. The enzymatic machinery is that of nonribosomal peptide synthetases (NRPSs), which use ATP-dependent aminoacylation logic to activate the particular amino acid selected as the aminoacyl-AMP. The thermodynamic activation is then utilized in a thiol-capture reaction to form an aminoacylthioester with retention of a significant fraction of the acyl group transfer potential. In NRPS assembly lines, the thioester activation drives peptide-bond formation as the nonribosomal peptide is elongated from a tandem series of aminoacyl-*S*-enzyme intermediates. The two domains in each NRPS module for amino acid selection and activation are the A and tethering PCP domains. The requisite thiol nucleophile in PCP domains is the post-translationally introduced phosphopantetheine prosthetic group (*24*, *25*).

Capture of the pyrrole from the L-pyrrolyl-*S*-PCP does not take place via an amine nucleophile to form an amide, but instead, the thermodynamically activated pyrrole carboxylate as a thioester sets up distinct outcomes. For pyoluteorin and undecylprodigiosin, this outcome is represented in the capture of the activated pyrrole by a carbon nucleophile (*7*), while in the case of clorobiocin and coumermycin, the pyrrolyl-*S*-PCP is captured by oxygen nucleophiles (i.e., the 3′-OH of the decorated noviosyl ring in the late stages of antibiotic maturation) (*8*−*10*). Because it is thermodynamically difficult to activate a free pyrrole-2-carboxylate, it is anticipated that it is biosynthesized as its activated form from L-proline. For this, the anticipated strategy is the conversion of L-proline to the pyrrole-2-carboxylate via a thioester intermediate, utilizing the NRPS activation and tethering logic.

Indeed, the Clo/CouN4 and -5 pairs are clear examples of a free-standing A domain and a PCP domain as separate subunits. The L-proline-specific A domains make L-prolyl-AMP intermediates and transfer them to the HS-pantetheinyl-*S*-PCP holo partner proteins to yield the L-prolyl-*S*-PCP covalent aminoacyl-*S*-protein species. The PCP protein platform may provide sequestration to enable kinetic stability to the iminoacyl thioester and also control reactivity by protein−protein interactions with partner proteins. Only the L-prolyl-*S*-PCP and not free L-proline is the substrate for enzymatic desaturation by the N3 flavoenzyme, probably reflecting both a protein-mediated recognition selectivity and the effect of the thioester linkage at lowering the chemical barrier for oxidation. Both effects would ensure that free proline pools, required for protein biosynthesis, are not diminished by oxidation to pyrrole-2-carboxylate.

In this study, we have detected the 12-kDa acyl-*S*-PCP, L-prolyl-*S*-CloN5, by ESI−FTMS analysis. Further, we have monitored its conversion by the flavoenzyme CloN3 to the −2- and −4-Da acyl-*S*-PCP product, again by direct ESI−FTMS interrogation. ESI−FTMS has a resolution capable of discerning 2-Da modifications with ease when full conversion is expected. The presence of −2 and −4 Da as a mixture with unoxidized acyl-*S*-PCP or low conversions (<20%) generates a mixture of overlapping isotopic distributions with the normal ^{13}C and ^{15}N content in proteins. The isotopic overlap is drastically reduced by depleting both ^{13}C and ^{15}N to narrow the isotopic envelope. This enables far more robust detection of low amounts of −2- and −4-Da changes on the acyl-*S*-protein in the presence of excess starting material. We used NH_3 depleted of ^{15}N and glucose depleted of ^{13}C as nitrogen and carbon sources, respectively, for *E. coli* to produce CloN5. Then, in addition, because the −2-Da intermediate forms transiently on its way to the −4-Da pyrrolyl-*S*-CloN5 product, we resorted to rapid quench studies followed by protein ESI−FTMS analysis to see substrate, intermediate, and product forms of the prolyl-, pyrrolinyl-, and pyrrolyl-*S*-protein. The detection of the intermediate and the pyrrolyl-*S*-ClonN5 establishes that the CloN3-mediated oxidation does occur in the anticipated tandem two-electron removal steps and that both steps are catalyzed by CloN3, presumably with 2 equiv of O_2 as reducible cosubstrate (if each O_2 is reduced to H_2O_2).

Flavoprotein enzymes are versatile oxidation biocatalysts. Some, such as the acyl CoA desaturases, dihydroorotate DH, and succinate DH, form conjugated olefins, by net C_α−H,C_β−H removal. Others, including D-amino acid oxidase (*26*), NikD (*27*, *28*), and ThiO (*29*, *30*) oxidize amino acid C−N bonds to the imino acids, removing C_α−H and N−H (Figure 9A). The first route in L-prolyl-*S*-CloN5 oxidation would yield a 2,3-dehydro-L-prolyl-*S*-PCP. The second route would yield the γ^2-pyrrolinyl-*S*-CloN5 acyl enzyme as the −2-Da intermediate. It is not clear which of these two regiospecific routes is the one that CloN3 follows in its first cycle, nor is it known if there is facile imine−enamine tautomerism that would equilibrate those −2-Da intermediate forms of the acyl-*S*-CloN5.

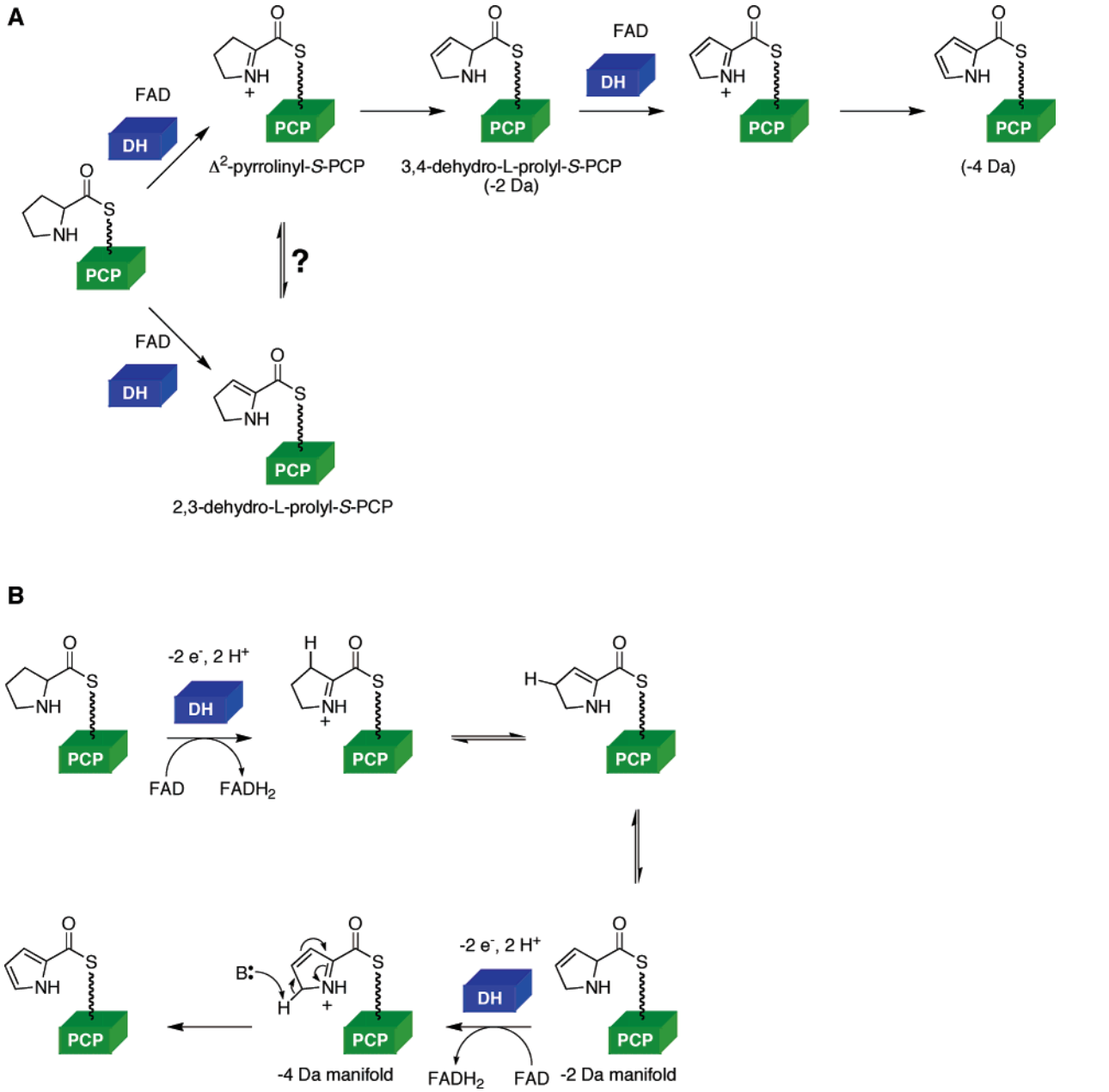

FIGURE 9: Mechanistic analysis for the oxidation of L-prolyl-*S*-CloN5. (A) Mechanistic analysis of the C−C versus C−N oxidation and mechanistic hypothesis for the oxidation of 3,4-dehydro-L-prolyl-*S*-CloN5 if CloN3 can oxidize the C2−N bond. (B) Mechanistic proposal for the formation of the pyrrolyl-*S*-CloN5 from L-prolyl-*S*-CloN5.

The experiments with 3,4-dehydro-L-proline show that this −2-Da regioisomer is processed by CloN4, installed on holo-CloN5, and oxidized by CloN3 to the −4-Da pyrrolyl-*S*-PCP product (Figure 9). Presumably, this aminoacyl-*S*-PCP is oxidized by CloN3 via the C−N oxidation pathway. It is oxidized some 8-fold faster than L-prolyl-*S*-PCP, making it a candidate for a kinetically competent intermediate. A unifying mechanism for CloN3 acting twice on L-prolyl-*S*-CloN5 to yield the pyrrolyl-*S*-CloN5 product would be two tandem C−N oxidations (Figure 9B). This would require that the −2-Da intermediate tautomerizes between imine−enamine (α,*β* double bond) and the deconjugated 3-dehydro-L-prolyl (*β*,*γ* double bond), which could be the substrate for the −2- to −4-Da step. There are enzymes known in bacterial fatty acid metabolism that carry out such α,*β*−*β*,*γ* isomerizations (*31*), but it remains to be seen if and how such equilibration occurs on the suite of dehydro-L-prolyl-*S*-PCP regiosiomers. The flavoenzyme NikD in nikkomycin biogenesis catalyzes analogous oxidation in picolinate formation (*28*).

The net result of the action of CloN3, -4, and -5 and by analogy CouN3, -4, and -5 is the sequestering of a fraction of the cellular pool of the proteinogenic amino acid L-proline and its four-electron oxidation to the heteroaromatic pyrrolyl-2-thioester on a free-standing PCP domain. The thioester linkage provides the requisite thermodynamic activation to enable pyrrolyl group transfer to the noviosyl sugar-3′-OH and to create the pharmacophore in this antibiotic class (Figure 1D). This work provides the protein thioester substrate needed to develop an assay for the pyrrolyltransferases Clo/CouN2, which in turn should allow for exploration of diversification of this heteroaromatic acyl moiety on the aminocoumarin antibiotic scaffolds of clorobiocin and coumermycin A_1.

ACKNOWLEDGMENT

We thank Professor Lutz Heide for the generous gift of plasmids containing the gene encoding for Clo/CouN3, -4, and -5. We also thank Michelle Pacholec for help with preliminary experiments.

REFERENCES

1. Nowak-Thompson, B., Chaney, N., Wing, J. S., Gould, S. J., and Loper, J. E. (1999) Characterization of the pyoluteorin biosynthetic gene cluster of *Pseudomonas fluorescens* Pf-5, *J. Bacteriol. 181*, 2166−2174.
2. Brodhagen, M., Henkels, M. D., and Loper, J. E. (2004) Positive autoregulation and signaling properties of pyoluteorin, an antibiotic produced by the biological control organism *Pseudomonas fluorescens* Pf-5, *Appl. Environ. Microbiol. 70*, 1758−1766.
3. Furstner, A. (2003) Chemistry and biology of roseophilin and the prodigiosin alkaloids: A survey of the last 2500 years, *Angew. Chem., Int. Ed. 42*, 3582−3603.
4. Tsao, S. W., Rudd, B. A., He, X. G., Chang, C. J., and Floss, H. G. (1985) Identification of a red pigment from *Streptomyces coelicolor* A3(2) as a mixture of prodigiosin derivatives, *J. Antibiot. 38*, 128−131.
5. Tsai, F. T. F., Singh, O. M. P., Skarzynski, T., Wonacott, A. J., Weston, S., Tucker, A., Pauptit, R. A., Breeze, A. L., Poyser, J. P., O'Brien, R., Ladbury, J. E., and Wigley, D. B. (1997) The high-resolution crystal structure of a 24-kDa gyrase B fragment from *E. coli* complexed with one of the most potent coumarin inhibitors, clorobiocin, *Proteins: Struct., Funct., Genet. 28*, 41−52.
6. Radl, S. (1990) Structure−activity relationships in DNA gyrase inhibitors, *Pharmacol. Ther. 48*, 1−17.
7. Thomas, M. G., Burkart, M. D., and Walsh, C. T. (2002) Conversion of L-proline to pyrrolyl-2-carboxyl-*S*-PCP during undecylprodigiosin and pyoluteorin biosynthesis, *Chem. Biol. 9*, 171−184.
8. Pojer, F., Li, S.-M., and Heide, L. (2002) Molecular cloning and sequence analysis of the clorobiocin biosynthetic gene cluster: New insights into the biosynthesis of aminocoumarin antibiotics, *Microbiology 148*, 3901−3911.
9. Wang, Z.-X., Li, S.-M., and Heide, L. (2000) Identification of the coumermycin A_1 biosynthetic gene cluster of *Streptomyces rishiriensis* DSM 40489, *Antimicrob. Agents Chemother. 44*, 3040−3048.
10. Xu, H., Wang, Z.-X., Schmidt, J., Heide, L., and Li, S.-M. (2002) Genetic analysis of the biosynthesis of the pyrrole and carbamoyl moieties of coumermycin A_1 and novobiocin, *Mol. Genet. Genomics 268*, 387−396.
11. Thomas, M. G., Burkart, M. D., and Walsh, C. T. (2002) Conversion of L-proline to pyrrolyl-2-*S*-PCP during undecylprodigiosin and pyoluteorin biosynthesis, *Chem. Biol. 9*, 171−184.
12. Quadri, L. E. N., Weinreb, P. H., Lei, M., Nakano, M. M., Zuber, P., and Walsh, C. T. (1998) Characterization of Sfp, a *Bacillus subtilis* phosphopantetheinyl transferase for peptidyl carrier protein domains in peptide synthetases, *Biochemistry 37*, 1585−1595.
13. Patrie, S. M., Charlebois, J. P., Whipple, D., Kelleher, N. L., Hendrickson, C. L., Quinn, J. P., Marshall, A. G., and Mukhopadhyay, B. (2004) Construction of a hybrid quadrupole/Fourier transform ion cyclotron resonance mass spectrometer for versatile MS/MS above 10 kDa, *J. Am. Soc. Mass Spectrom. 15*, 1099−1108.
14. Senko, M. W., Canterbury, J. D., Guan, S., and Marshall, A. G. (1996) A high-performance modular data system for Fourier transform ion cyclotron resonance mass spectrometry, *Rapid Commun. Mass Spectrom. 10*, 1839−1844.
15. Ge, Y., Lawhorn, B. G., ElNaggar, M., Strauss, E., Park, J.-H., Begley, T. P., and McLafferty, F. W. (2002) Top down characterization of larger proteins (45 kDa) by electron capture dissociation mass spectrometry, *J. Am. Chem. Soc. 124*, 672−678.
16. Goeghegan, K. F., Dixon, H. B. F., Rosner, P. J., Hoth, L. R., Lanzetti, A. J., Borzilleri, K. A., Marr, E. S., Pezzullo, L. H., Martin, L. B., LeMotte, P. K., McColl, A. S., Kamath, A. V., and Stroh, J. G. (1999) Spontaneous α-*N*-6-phosphogluconoylation of a "His tag" in *Escherichia coli*: The cause of extra mass of 258 or 178 Da in fusion proteins, *Anal. Biochem. 267*, 169−184.
17. LeDuc, R. D., Taylor, G. K., Kim, Y.-B., Januszyk, T. E., Bynum, L. H., Sola, J. V., Garavelli, J. S., and Kelleher, N. L. (2004) ProSight PTM: An integrated environment for protein identification and characterization by top−down mass spectrometry, *Nucleic Acids Res. 32*, W340−W345.
18. Lambalot, R. H., Gehring, A. M., Flugel, R. S., Zuber, P., LaCelle, M., Marahiel, M. A., Reid, R., Khosla, C., and Walsh, C. T. (1996) A new enzyme superfamily−The phosphopantetheinyl transferases, *Chem. Biol. 3*, 923−936.
19. Quadri, L. E., Weinreb, P. H., Lei, M., Nakano, M. M., Zuber, P., and Walsh, C. T. (1998) Characterization of Sfp, a *Bacillus subtilis* phosphopantetheinyl transferase for peptidyl carrier protein domains in peptide synthetases, *Biochemistry 37*, 1585−1595.
20. Weinreb, P. H., Quadri, L. E., Walsh, C. T., and Zuber, P. (1998) Stoichiometry and specificity of *in vitro* phosphopantetheinylation and aminoacylation of the valine-activating module of surfactin synthetase, *Biochemistry 37*, 1575−1584.
21. Xu, H., Kahlich, R., Kammerer, B., Heide, L., and Li, S. M. (2003) CloN2, a novel acyltransferase involved in the attachment of the pyrrole-2-carboxyl moiety to the deoxysugar of clorobiocin, *Microbiology 149*, 2183−2191.
22. Roy, R. S., Gehring, A. M., Milne, J. C., Belshaw, P. J., and Walsh, C. T. (1999) Thiazole and oxazole peptides: Biosynthesis and molecular machinery, *Nat. Prod. Rep. 16*, 249−263.
23. Chen, H., Thomas, M. G., O'Connor, S. E., Hubbard, B. K., Burkart, M. D., and Walsh, C. T. (2001) Aminoacyl-*S*-enzyme intermediates in β-hydroxylations and α,β-desaturations of amino acids in peptide antibiotics, *Biochemistry 40*, 11651−11659.
24. Marahiel, M. A., Stachelhaus, T., and Mootz, H. D. (1997) Modular peptide synthetases involved in nonribosomal peptide synthesis, *Chem. Rev. 97*, 2651−2674.
25. Walsh, C. (2003) *Antibiotics: Action, Origins, Resistance*, 1st ed., ASM Press, Washington, DC.
26. Umhau, S., Pollegioni, L., Molla, G., Diederichs, K., Welte, W., Pilone, M. S., and Ghisla, S. (2000) The X-ray structure of D-amino acid oxidase at very high-resolution identifies the chemical mechanism of flavin-dependent substrate dehydrogenation, *Proc. Natl. Acad. Sci. U.S.A. 97*, 12463−12468.
27. Venci, D., Zhao, G., and Jorns, M. S. (2002) Molecular characterization of NikD, a new flavoenzyme important in the biosynthesis of nikkomycin antibiotics, *Biochemistry 41*, 15795−15802.
28. Bruckner, R. C., Zhao, G., Venci, D., and Jorns, M. S. (2004) Nikkomycin biosynthesis: Formation of a 4-electron oxidation product during turnover of NikD with its physiological substrate, *Biochemistry 43*, 9160−9167.
29. Settembre, E. C., Dorrestein, P. C., Park, J.-H., Augustine, A. M., Begley, T. P., and Ealick, S. E. (2003) Structural and mechanistic studies on ThiO, a glycine oxidase essential for thiamin biosynthesis in *Bacillus subtilis*, *Biochemistry 42*, 2971−2981.
30. Park, J.-H., Dorrestein, P. C., Zhai, H., Kinsland, C., McLafferty, F. W., and Begley, T. P. (2003) Biosynthesis of the thiazole moiety of thiamin pyrophosphate (vitamin B1), *Biochemistry 42*, 12430−12438.
31. Bloch, K. (1972) The enzymes, in *The Enzymes* (Boyer, P., Ed.) 3rd ed., Vol. 5, p 441, Academic Press, New York.

BI0476329